Asian Journal of Chemistry; Vol. 31, No. 10 (2019), 2157-2164

ASIAN JOURNAL OF CHEMISTRY

https://doi.org/10.14233/ajchem.2019.22028

Synthesis, Characterization and *in vitro* Antimicrobial Evaluation of Chalconeimine Derivatives as Potential Inhibitors against Enzymes Produced from *S. aureus*: A Computational Approach

B. PRITHIVIRAJAN[1], M. JEBASTIN SONIA JAS[1,2] and G. MARIMUTHU[3,*]

[1]Research and Development Centre, Bharathiar University, Coimbatore-641046, India
[2]Department of Chemistry, IFET College of Engineering, Villupuram-605108, India
[3]Department of Chemistry, Swami Dayananda College of Arts and Science, Manjakkudi-612610, India

*Corresponding author: E-mail: gmarimuuthu@gmail.com

Received: 25 February 2019; *Accepted*: 13 April 2019; *Published online*: 30 August 2019; AJC-19516

(Z)-1-(Benzo[*d*][1,3]dioxol-5-yl)-3-(4-(difluoromethoxy)-3-hydroxyphenyl)prop-2-en-1-one hydrazone derivatives pronounced in this manuscript represents a new collection of antibacterial agents in addition to the DNA gyrase inhibitors. Efforts had been made to synthesize those chalcone-hydrazone derivatives (**4a-e**) in good yields. The literature survey confirms that nano-ZnO as heterogeneous catalyst has obtained big interest because of its ecofriendly nature and has been explored as a effective catalyst for several organic ameliorations. Subsequently, induced by way of these observations and in continuation to our interest in organic synthesis with using nanocatalyst. *in vitro* Antibacterial activity has been evaluated towards Gram-positive and Gram-negative bacterial strains for all compounds. So one can discover the affinity to bacterial proteins docking have a look at have been carried out for 5 synthesized derivatives, antibiotic drug and co-crystallized ligands with special mechanism of action DNA gyrase B and methylthioadenosine/S-adenosylhomocysteine nucleosidase (MTAN) the usage of AutoDock 4.

Keywords: Hydrazone, Chalcone, Antibacterial, Docking, DNA gyrase B, Methylthioadenosine.

INTRODUCTION

Chalcones and its derivatives show numerous organic activities. Chalcones are medicinally critical course of materials. It's also used as most important intermediate for synthesis of heterocyclic compounds like pyrazolines, isoxazolines, flavonone, pyrimidines and so forth. They have virtually been said to possess biological behaviour like antioxidant [1], antimalarial [2], analgesic [3], anti-inflammatory [4], anticancer [5], insecticidal [6], antibacterial activity [7], fungicidal [8] activities. Currently, it's far simply one of the reliable computational method to pick out the interplay of two molecules, forecast the interplay power in among two molecules as well as to locate the most effective alignment of ligand with receptor molecule. It moreover offers honestly useful information regarding the affinity and additionally pastime of the tiny molecule on the goal proteins. Microorganisms have surely recognized before hand proper into presence more than 3.5 billion years ago [9]. Efficient healing options to combat *Staphylococcus aureus* infection are nevertheless restricted. And this makes a main burden to govern *Staphylococcus aureus* [10]. *S. aureus* is a commensally Gram-nice bacterium, which colonizes in human nasal mucosa either permanently or transiently [11], causing extreme infections ultimately [12,13]. However the medical signs aren't visualized until the immune device is affected [14]. But, the predominant trouble in controlling the *S. aureus* contamination is the incidence of multi-drug resistance produced specially because of the misuse of antibiotics. That is also as a result of the treatment of non-bacterial infections with antibiotics or inadequate compliance with the guidelines for drug ingestion. Consequently, new healing molecule is an urgence to be delivered as antibiotic inside the remedy of multi-drug resistant *S. aureus*. Treatment for *S. aureus* infection encountered several roadblocks because of high stage of penicillin, vancomycin and Methicillin resistance [15]. For this reason, there is a needful for developing new anti-staphylococcal marketers. The enzymes DNA gyrase B and methylthioadenosine/S-adenosylhomocysteine nucleosidase (MTAN) are found in bacteria and absent in

humans thereby appearing as a potential target in treating the *S. aureus* associated sicknesses. DNA gyrase is a type II topoisomerase that catalyzes the terrible supercoiling of DNA in prokaryotes. It supercoils DNA *via* a system of strand breakage/resealing and DNA wrapping [16]. Its function is essential to DNA replication, transcription and bacteriophage λ integrative recombination [17,18]. Its capacity to negatively supercoil a comfortable plasmid DNA substrate is precise consequently serving as a goal for antimicrobial pills.

MTAN has currently been determined and it's miles concerned in the quorum sensing pathway of microorganism [19]. Inhibition of MTAN prevents the catalyzing mechanism had to produce autoinducers that's important for the bacterial cells to sense the presence of its population. MTAN additionally catalyzes the irreversible cleavage of the glycosidic bond in 5'-methylthioadenosine (MTA) and S-adenosylhomocysteine (SAH) [20]. Inhibition of MTAN leads to aggregation of MTA and SAH substrates which in flip inhibits crucial biological strategies in microorganism like polyamine synthesis, methylation, bacterial quorum sensing and methionine recycling [21]. Subsequently, the absence of MTAN enzyme in mammalian species and its vital position in microorganism has implicated this as a target for antimicrobial drug layout [22,23]. In chalconeimine synthesis, most of the techniques have treasured advantages, which include moderate response situations, accurate yields and no undesirable byproducts. The period of the pronounced method as well as yields is not sufficiently accurate. So, regardless of the aforementioned advantages of this technique, we determined to sell some elements of this studies which includes the reactivity of substrates. Therefore, we carried out the reactions the usage of zinc oxide nanoparticles as green catalysts.

The current literature survey famous that nano-ZnO as heterogeneous catalyst has obtained enormous interest due to its ecofriendly nature and has been explored as a effective catalyst for several natural changes [24]. As a result, precipitated by means of those observations and in continuation to our hobby in organic synthesis with the usage of nanocatalyst [25], we record a clean and rapid catalytic software of ZnO nanoparticles for one-pot synthesis of hydrazone derivatives incorporating methylene dioxy moiety.

EXPERIMENTAL

Thin layer chromatography (TLC) became used to check the progress and final touch of the response the usage of silica gel G as an adsorbent (stationary phase) and ethyl acetate and hexane as cell phase. Open glass capillaries were used to determine the melting factor on famous melting point apparatus and had been uncorrected. ^{1}H and ^{13}C nuclear magnetic resonance spectra were recorded on Bruker Avance II 400 NMR spectrometer (400 MHz) at 298 K, in suitable deuterated solvent. Chemical shift were mentioned as δ (ppm) relative to tetramethyl silane (TMS) as internal popular. Infrared spectra (IR) had been recorded as KBr pellet on Shimadzu toes-IR spectrometer.

Docking studies: X-ray crystal structures of DNA gyrase B (PDB Id: 3G7B) and 5'-methylthioadenosine/S-adenosylhomocysteine nucleosidase [MTAN] (PDB identity: 3BL6) were retrieved from the Protein Data Bank [26]. The docking research has been achieved the use of crystal structure of DNA gyrase of *S. aureus* (PDB Id: 3U2D) retrieved from the Protein Data Bank. To put together the receptor for docking studies, cocrystallized ligand and water molecules were eliminated, at the same time as polar hydrogen atoms and Kollman-united costs have been protected to the DNA gyrase receptor molecules. The essential pdb and pdbqt documents of ligands and *S. aureus* DNA gyrase receptor were prepared the usage of AutoDock 4.2 software [27]. The observe become finished the use of the usual docking protocol applied for AutoDock Vina in PyRx 0.8 software [28]. The docking consequences were analyzed using Discovery Studio four.Zero (Accelrys, Inc. San Diego, CA 92121, U.S.).

Anibacterial activity: All of the synthesized chalconeimine derivatives (**4a-e**) had been tested for their antibacterial interest towards a bacterial strain, specifically, *Staphylococcus aureus* with the aid of paper disc diffusion method with various concentrations of the derivatives prepared in dimethyl sulfoxide. The reason of choosing DMSO for antibacterial research become that it has no impact at the above referred to bacterial strains [29]. Nutrient agar used as the tradition medium for the growth of bacterial colony that turned into organized by the usage of peptone (3.0 g), NaCl (3.0 g), yeast (1.5 g), agar (6.0 g) in 300 mL of distilled water with pH at 7.00. The prepared medium is autoclaved at 15 pa for 20 min and kept at a 120 °C for 30 min to sterilize the media. This media became then poured into petri-dishes slowly in laminar go with the flow surroundings, allowed to solidify and stored at 30 °C for 24 h [30]. The bacterial lines have been inoculated by means of spreading in peptidases and its temperature is maintained at 30 °C for 24 h. The usage of paper disc (8 mm) in nutrient agar medium, exclusive concentrations (50, 100, 150 µg/mL) of the newly synthesized chalcone imines (**4a-e**) were loaded *via* bacteria unfastened micro pipettes. The antibacterial activity changed into determined by means of measuring the zone of inhibition in millimeters and as compared with standard drug amoxicellin and cefixime.

Synthesis of ZnO nanoparticles: Natural ZnO turned into organized through hydrolysis and oxidizing method. $Zn(NO_3)_2$ (1 mmol) dissolved in 100 mL of distilled water with continuous stirring. NaOH was added into brought into the former solution drop by drop until the pH of the answer became 12. White precipitate were washed 3 times with distilled water and dried for 24 h at 80 °C.

General procedure for the synthesis of (*E*)-1-(4-(difluoromethoxy)-3-hydroxyphenyl)-3-phenylprop-2-en-1-one (3): 4-(Difluoromethoxy)-3-hydroxybenzaldehyde (**1**, 0.02 mol) and 1-(benzo[*d*][1,3]dioxol-5-yl)ethanone (**2**, 0.02 mol) have been dissolved in 30 mL of alcohol. To this reaction mixture 40 % NaOH (10 mL) and ZnO nanoparticles catalyst (0.003 g), in ethanol (5 mL) had been introduced. The development of the reaction become accompanied through TLC. After completion of the reaction, the combination became filtered to remove the catalyst and the filtrate turned into taken in ether, washed with water and dried over anhydrous sodium sulfate. Elimination of solvent gave the crude product which changed into

recrystallized from methanol. m.p.: 96 °C; m.f.: $C_{17}H_{12}O_5F_2$; m.w.: 334.

General procedure for the synthesis of 5-((1Z,3Z)-3-(benzo[*d*][1,3]dioxol-5-yl)-4-(substituted pyridin-2-yl)buta-1,3-dien-1-yl)-2-(difluoromethoxy)phenol (4a-e): (E)-1-(4-(Difluoromethoxy)-3-hydroxyphenyl)-3-phenylprop-2-en-1-one (**3**, 0.01 mol) and substituted aniline (0.01 mol) was dissolved in ethanol (20 mL). To this mixture ZnO nanoparticles was added and it was refluxed for 3 h. On cooling and dilution with ice cold water, a solid mass separated out. It was recrystallized from ethanol (**Scheme-I**). The physical data of the synthesized compounds are given in Table-1.

TABLE-1
PHYSICAL DATA OF VARIOUS SYNTHESIZED COMPOUNDS

Compd.	Colour	m.f.	m.w.	Solubility	m.p. (°C)
4a	Yellow	$C_{22}H_{15}N_2O_4ClF_2$	444	Ethanol	157
4b	Yellow	$C_{22}H_{15}N_2O_4ClF_2$	444	Ethanol	133
4c	Yellow	$C_{22}H_{15}N_2O_4ClF_2$	444	Ethanol	148
4d	Pale yellow	$C_{23}H_{18}N_2O_4F_2$	424	Ethanol	128
4e	Pale yellow	$C_{23}H_{18}N_2O_4F_2$	424	Ethanol	118

RESULTS AND DISCUSSION

UV visible absorption spectra had been examined with the aid of dispersing nano catalyst in the high purity at room temperature (Fig. 1). The UV absorption for plant mediated synthesized ZnO observed in wavelength 377 nm. Which is ideal settlement with the preceding paintings [31]. Fig. 2 suggests XRD diffraction sample of ZnO nanoparticles. It's miles located that there exist sturdy diffraction height with 2θ values of 31.73°, 36.23°, 47.48°, 56.58°, 62.83° and 67.88°. Similar to the crystal planes of (100), (101), (102), (110), (103) and (112), respectively. All diffraction peaks of sample correspond to the characteristic hexagonal wurtzite shape of zinc oxide nanoparticles. Similar, X-ray diffraction sample become reported *via* Culity *et al.* [32] and Bhattacharyya *et al.* [33]. The use of the Scherer equation [34] the common crystalline length of ZnO nanoparticles is found to be 20 nm. Diffraction pattern similar to impurities are determined to be absent. This proves that pure ZnO nanoparticles had been synthesized. Hence the morphology and length of the ZnO nanoparticles had been analyzed with the aid of scanning electron microscope. SEM photograph had proven character ZnO nanoparticles in

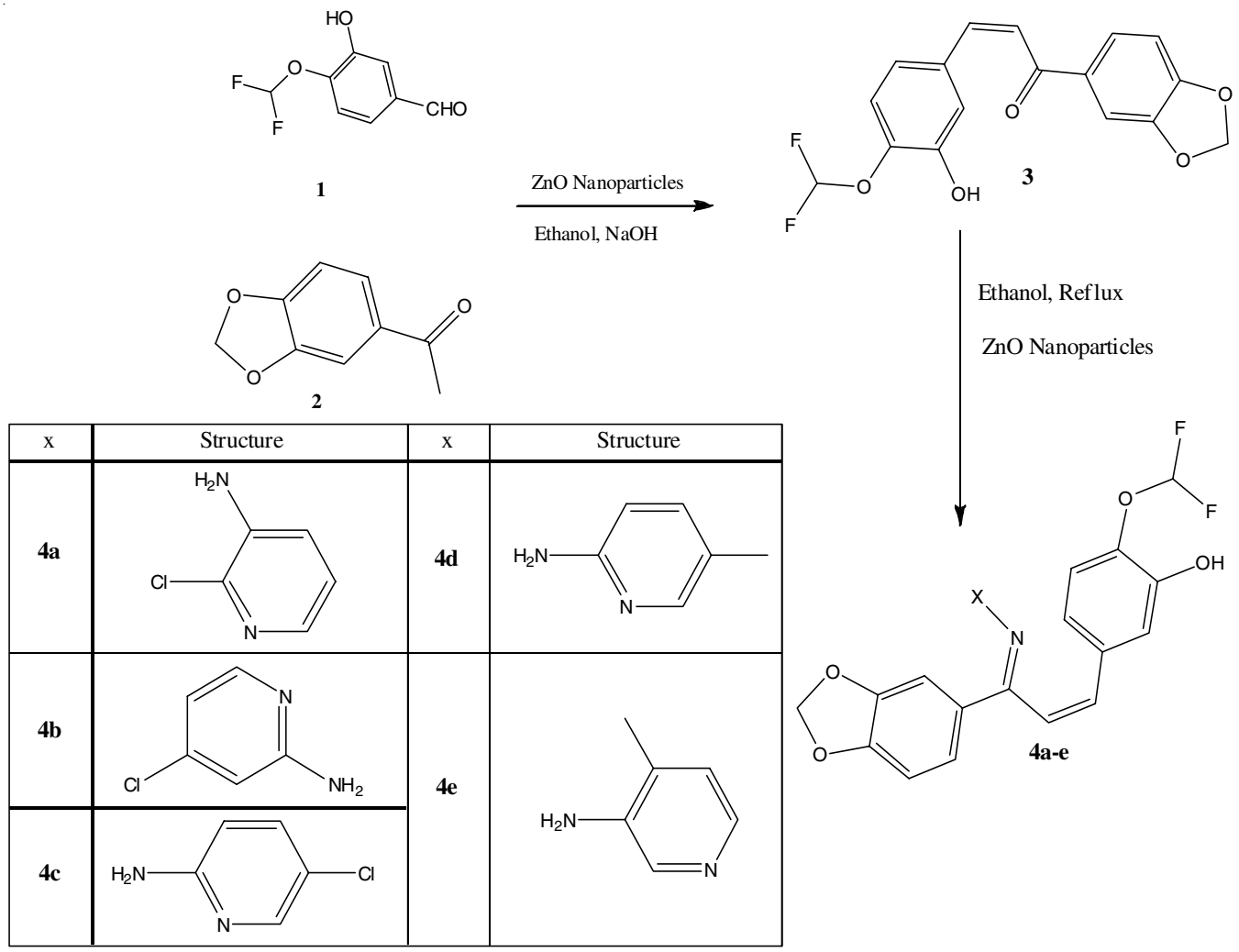

Scheme-I: Synthesis of 5-((1Z,3Z)-3-(benzo[*d*][1,3]dioxol-5-yl)-4-(substituted pyridin-2-yl)buta-1,3-dien-1-yl)-2-(difluoromethoxy)phenol (**4a-e**)

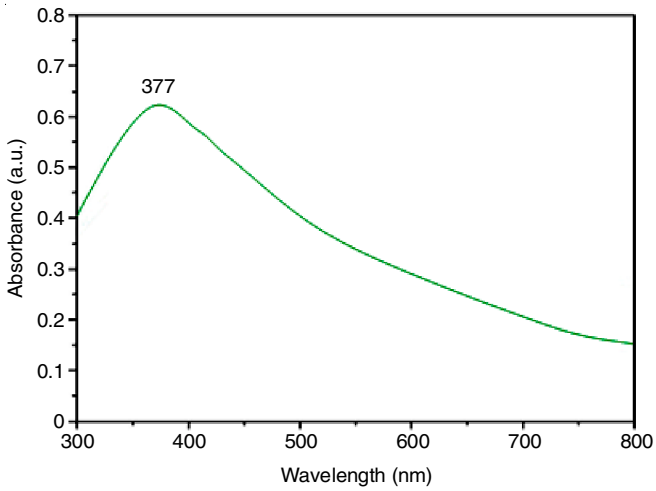

Fig. 1. UV-visible absorption spectrum of ZnO nanoparticles

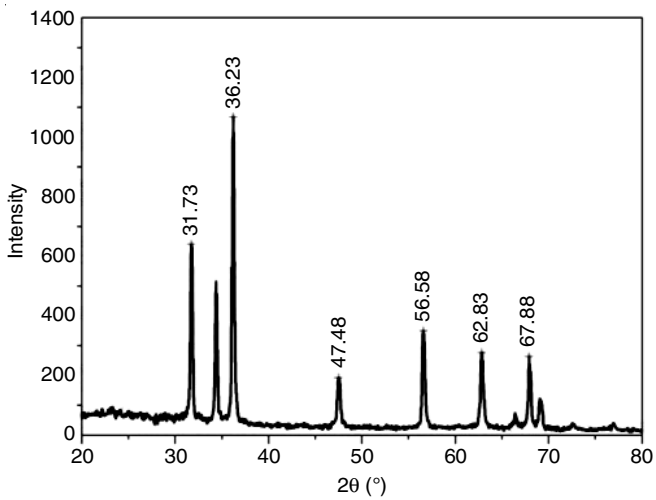

Fig. 2. XRD pattern of bio derived ZnO nanoparticles

addition to range of aggregates. Fig. 3a illustrates the particles are predominantly round in shape and aggregates into larger particles without a well-defined morphology The chemical purification of samples as well as their stoichiometry changed into tested through EDX studies. As proven Fig. 3b zinc and oxygen are the most effec-tive fundamental additives of the prepared nanoparticles.

In FT-IR spectrum of ZnO nanoparticles, the band at 619 cm^{-1} is assigned to the stretching vibrations of (Zn–O) bond. The broad band with low intensity at 3448 cm^{-1} is associated to vibration mode of (OH) group, representing the being there of little quantity of water adsorbed on the ZnO nanoparticles surfaces.

The IR frequencies of compounds **4a-e** are showed in Table-2 in which the C=N stretching frequency come out at 1667-1586 cm^{-1} aromatic (CH) stretching frequencies appear at 3093-3084 cm^{-1} and stretching frequency observed at 1666-1625 cm^{-1} C=O group there in the derivatives.

TABLE-2
IR SPECTRA OF CHALCONEIMINE DERIVATIVES (**4a-e**)

Compd.	Frequency (ν_{max}, cm^{-1})				
	C=O	C=N	Ali C-H	CH=CH	arom C-H
4a	1666	1597	2966	1452	3089
4b	1645	1586	2924	1425	3084
4c	1645	1589	2924	1448	3084
4d	1625	1586	2926	1452	3093
4e	–	1667	2924	1450	3088

The ^1H NMR chemical shift values of compounds (**4a-e**) are given in Table-3. The singlet observed in the range 6.30-6.60 ppm is owing $–CH_2$ methylene proton of 3',4'-methylene-dioxy acetophenone moiety proton. The singlet observed at 7.41-7.49 ppm is due –CH proton of $–CHF_2$ moeity. The signals appearing 7.14-8.38 ppm are apparently owing to aromatic protons.

The three dimensional X-ray structures of DNA gyrase B (PDB ID: 3G7B) and MTAN (3BL6) of *S. aureus*, retrieve from the Protein Data Bank are shown in Figs. 4 and 5 along with its active site residues. DNA gyrase B and MTAN were solved in complex with its particular inhibitors specifically, methyl ((5-(4-(4-hydroxypiperidin-1-yl)-2-phenylthiazol-5-yl)-1*H*-pyrazol-3-yl)methyl)carbamate and formycin A.

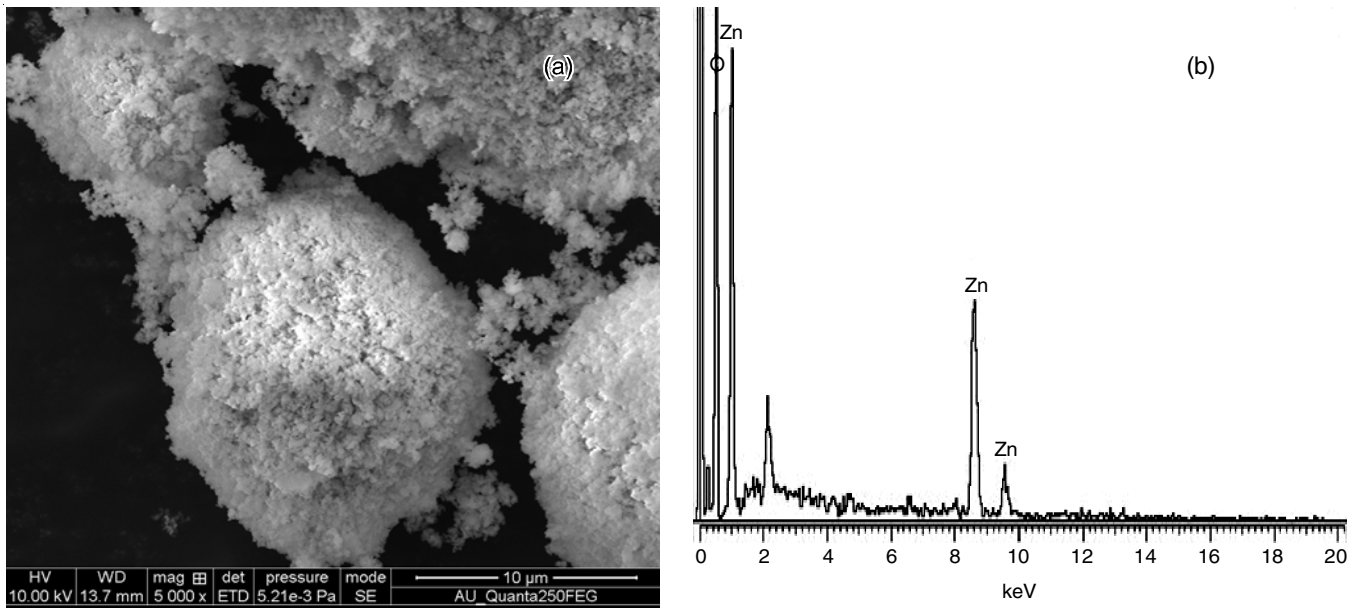

Fig. 3. SEM image (a) and EDX (b) of bio derived ZnO nanoparticles

TABLE-3
^{1}H NMR SPECTRA OF HYRAZONE DERIVATIVES (**4a-e**)

Compounds	-CH_2	CHF_2	Aromatic protons
4a	6.30 (2H, singlet)	7.48 (1H, singlet)	7.43-8.36 (11H, multiplet)
4b	6.60 (2H, singlet)	7.47(1H, singlet)	7.47-7.95 (11H, multiplet)
4c	6.55 (2H, singlet)	7.49 (1H, singlet)	7.43-8.38 (11H, multiplet)
4d	6.58 (2H, singlet)	7.46 (1H, singlet)	7.28-7.96 (11H, multiplet)
4e	6.55 (2H, singlet)	7.41 (1H, singlet)	7.14-8.38 (11H, multiplet)

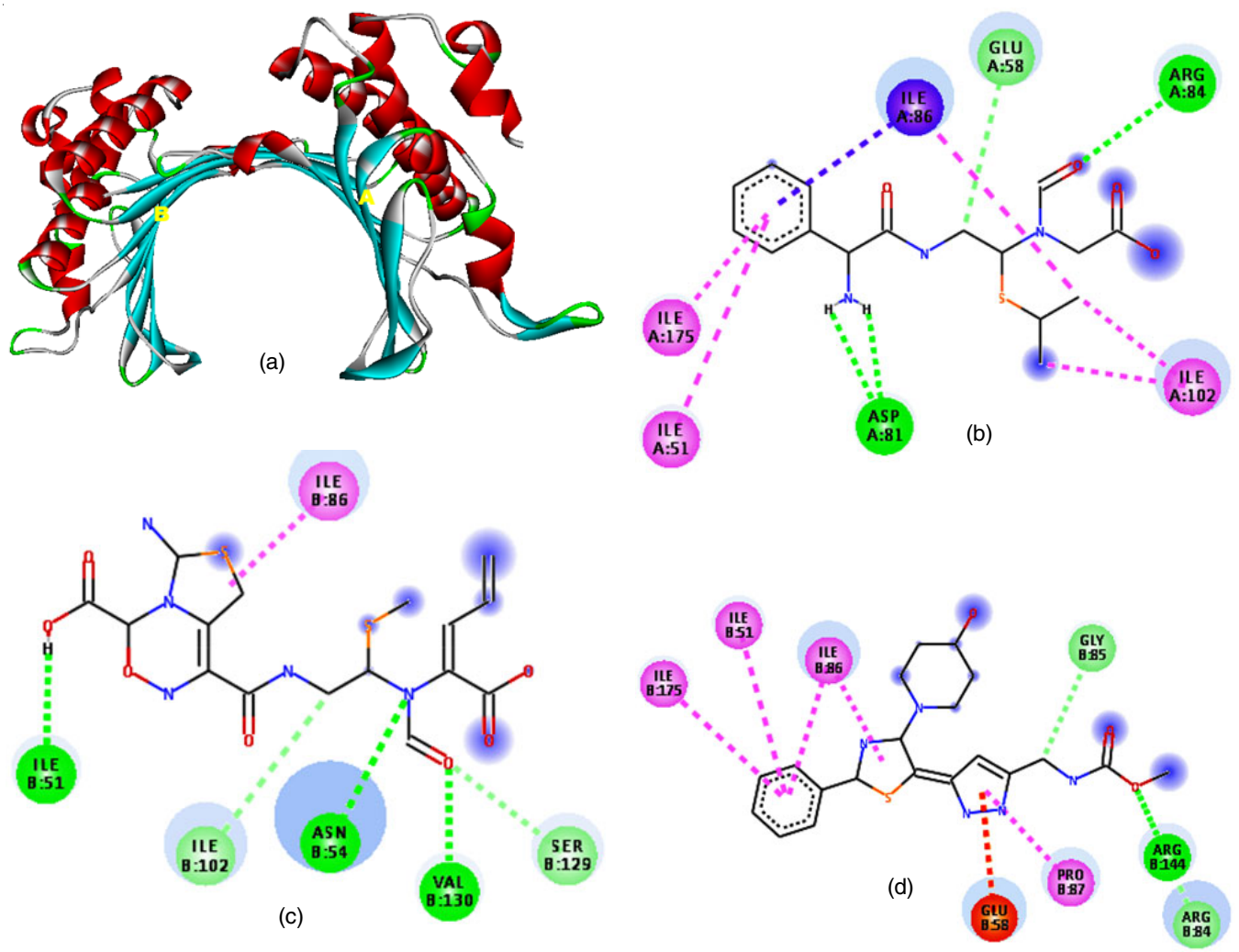

Fig. 4. (a) DNA gyrase B of *S. aureus*; (b) Binding pose of amoxicillin with DNA gyrase B; (c) Binding pose of cefixime with DNA gyrase B; (d) Binding pose of co-crystal structure ligand with DNA gyrase B

These complex structures of the inhibitor and the protein and these interactions are taken as the reference for the chalconeimine derivative (**4a-e**). The co-crystallized ligand forms the hydrogen bond interaction with the residues GLY 85, ARG 144 and ARG 84 (Figs. 4 and 5) which are there within the ATP binding pocket. The ligand is well additional stabilized by a number of hydrophobic contacts with the residues ILE 175, ILE 51, ILE 86, GLU 58 and PRO 87. The co-crystallized ligand of MTAN forms several hydrogen bonds with the residues of SER 75, ASP 196, MET 172, VAL 170, GLU 11 and GLU 173 (Table-4).

The docking studies clearly make known that some of these compounds bind proficiently to the enzymes produced from *S. aureus*. Binding score of Autodock 4.2 vary between -8.1 to -8.8 for compounds **4a-e** tested for DNA gyrase B and -7.3 to -7.7 for MTAN (Table-5). Out of the five chalconeimine derivatives analyzed, compound **4a** forms the best interaction with DNA gyrase B and MTAN, respectively.

The compound **4a** has the highest binding score of -8.8. The hydrogen atom on pyridine ring forms hydrogen bond with the oxygen atom of ILE 51, SER 55 and ASP 81 (Fig. 4). Compound **4b** and **4e** having a binding score of -8.5 makes hydrogen bonds with the active site residue GLU 58 of DNA gyrase B (Fig. 4). The hydrogen atom on pyridine ring of compound **4a** forms a hydrogen bond with the side chain carboxylate group of GLU 58 (Fig. 4). Hydrogen bond pattern are different for these two compounds. Re-docking of the inhibitor from the co-crystallized complex structure (Fig. 4) of DNA gyrase

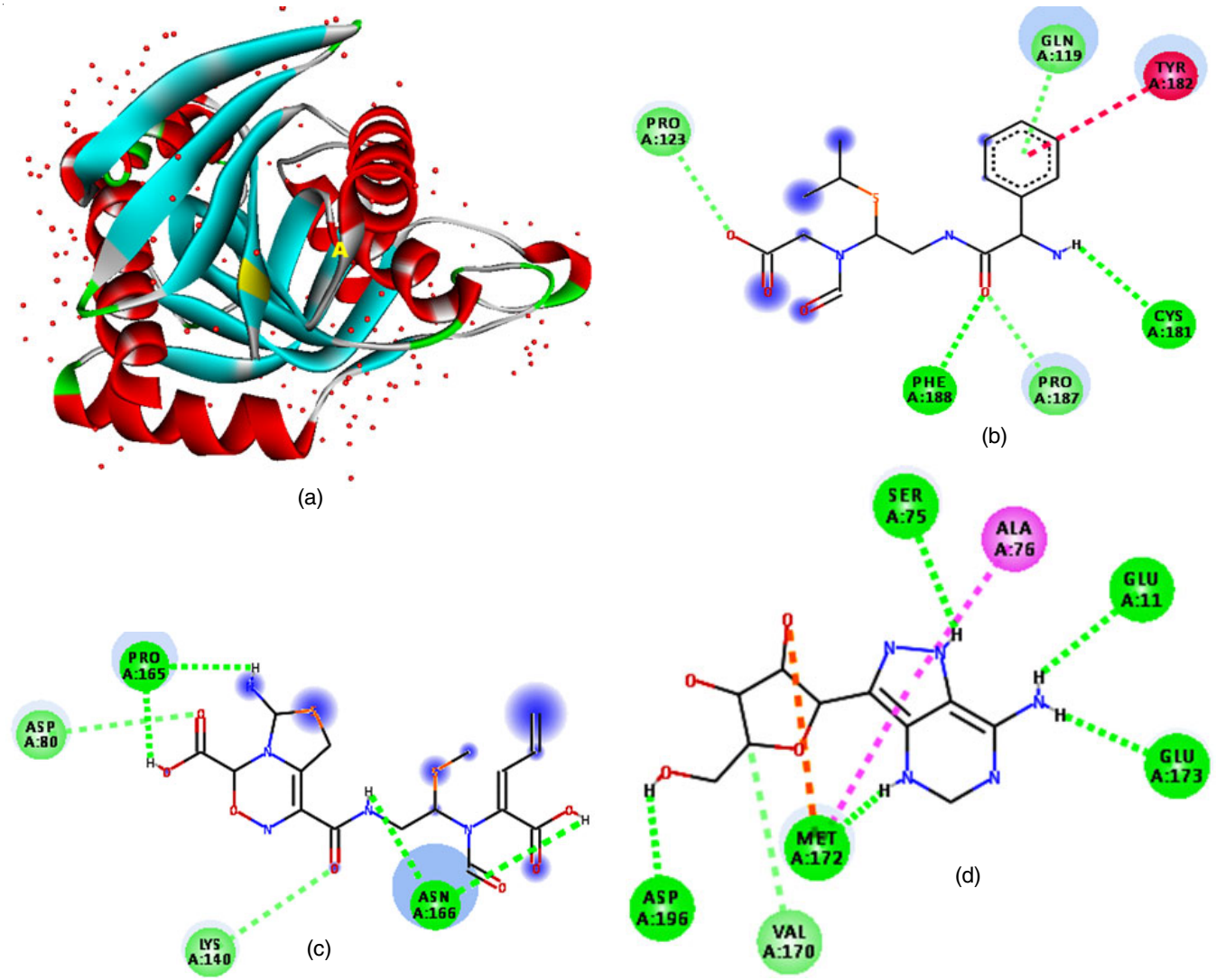

Fig. 5. (a) MTAN of *S. aureus*; (b) Binding pose of amoxicillin with MTAN; (c) Binding pose of cefixime with MTAN; (d) Binding pose of co-crystal formycin ligand with MTAN

TABLE-4
INTERACTION PATTERN OF CHALCONEIMINE DERIVATIVES (**4a-e**) WITH DNA GYRASE B AND MTAN PROTEIN

Compounds	DNA gyrase B		MTAN	
	Hydrogen bond interaction	Other interaction	Hydrogen bond interaction	Other interaction
4a	PHE 188, ALA 117,GLN 119	PRO 115	ILE 51, SER 55, ASP 81,ARG 144	ILE 102, GLU 58, ARG 84, PRG 87
4b	ALA 128, ALA 117	PRO 115, GLN 119, SER 120, VAL 116	GLU 58	ARG 84, ILE 86, PRO 87
4c	ALA 117, ASN 185	GLN 119, CYS 181, TYR 182, VAL 116, PRO 115, VAL 186		ILE 86, ASP 57, ARG 84, PRO 87
4d	PHE 188, ALA 178	VAL 116, ALA 117, GLN 119, PRO 187, VAL 186	ARG 144, ASP 81, THR 173	ILE 51, ILE 86, PRO 87, ILE 102, ARG 84
4e	CYS 181	ALA 178, SER 121, PRO 123, PRO 187, GLN 119	GLU 58	ARG 84, PRO 87, ILE 86, ALA 61
Amoxillin	GLN 119, CYS 181, PRO 187, PHE 188, PRO 123	TYR 182	GLU 58, ASP 81, ARG 84	ILE 175, ILE 51, ILE 102
Cifixime	PRO 165, ASP 80, ASN 166, LYS 140		ILE 51, ILE 102, ASN 54, VAL 130, SER 129	ILE 86
Co-crystallized ligand	SER 75, ASP 196, MET 172, VAL 170, GLU 11, GLU 173	ALA 76	GLY 85, ARG 144, ARG 84	ILE 175, ILE 51, ILE 86, GLU 58, PRO 87

B resulted in a binding score of -8.1 which is comparable to the scores found for compound **4a**, **4b** and **4e**. The re-docked conformation of co-crystallized ligand (Fig. 4) resembles the conformation of chalconeimine derivatives (compound **4a**, **4b** and **4e**, respectively).

TABLE-5
BINDING SORES OF THE CHALCONEIMINE COMPOUNDS WITH DNA GYRASE B AND MTAN OF *S. aureus*

Compounds	DNA gyrase B	MTAN
4a	-8.8	-7.7
4b	-8.5	-7.7
4c	-8.1	-7.6
4d	-8.1	-7.6
4e	-8.5	-7.3
Amoxicillin	-6.7	-6.9
Cefixime	-7.0	-6.5
Co-crystallized ligand	-8.1	-6.7

We also analyzed the interaction and energy profile of DNA gyrase B with the amoxicillin and cefixime (Fig. 4). The docking of amoxillin and cefixime with DNA gyrase B of *S. aureus* resulted in a binding score of -6.7 and -7.0, which is less binding energy than compound **4a**, **4b** and **4e**.

The compound **4a** and **4b** form the best interactions with MTAN of *S. aureus*. The compound **4a** form hydrogen bonds with PHE 188, ALA 117 and GLN 119 of MTAN with the binding score of -7.7. Apart from this, hydrophobic interactions are observed between the compound **4a** with PRO 115 and compound **4b** with PRO 115, GLN 119, SER 120 and VAL 116 which also contributes to the stability of this complex. The compound **4b** form hydrogen bonds with ALA 117 and ASN 185 of MTAN with the binding score of -7.7.

The MTAN compound **4b** complex is mostly stabilized by hydrophobic and van der Waals interactions resulting in a binding score of -7.7. In order compare the binding mode of chalconeimine derivative with the already established inhibitor for this enzyme, formycin A. The docking results showed that present compounds also bind with MTAN produced from *S. aureus* in a almost similar way as like formycin A. (binding score -6.7).

We also analyzed the interaction and energy profile of MTAN with the already available drug amoxillin and cefixime (Fig. 5). The docking of amoxillin and cefixime with MTAN of *S. aureus* resulted in a binding score of -6.9 and -6.5, which is less binding score results found for compound **4a** and **4b**.

All the synthesized compounds were studied for their antibacterial activity against clinically isolated Gram-positive strains *S. aureus* using conventional disc diffusion method. The minimum inhibitory concentration (MIC) values were calculated by comparison to amoxicillin and cefixime as the reference bacterial drug and they are shown in Table-6. Compounds **4a-e** have shown antibacterial activity with MIC value in the range of 100 µg/mL against Gram-positive *S. aureus*. Compounds **4a**, **4b** and **4e** have shown antibacterial activity with MIC value in the range of 50 µg/mL against Gram-positive *S. aureus*. In terms of structure activity relationship, results suggest that compounds having chloro and methyl on pyridine ring at C-2, 3 and 5 exhibited the most potent antibacterial activity. GyrB has been proposed as the main binding target for antibacterial activity [35]. Molecular docking described an explanation for the mechanism for synthesized derivatives antibacterial activities by illustrating the interaction between chalconeimine with GyrB and MTAN. From the docking study we predicted that chalconeimine analogues (**4a-e**) possess better antibacterial activity equal to the standard drugs by having good binding affinity with target protein and it could be used as potential drug as antimicrobial. Amongst all the docked compounds, compound **4a**, **4b** and **4e** shows good binding affinity and interaction with DNA gyrase and MTAN enzymes with reference to amoxicillin and cefixime. It was found that the predicted docking results using Autodock 4 software were quite accurate after comparing it with the actual antimicrobial activity.

TABLE-6
MINIMUM INHIBITORY CONCENTRATIONS (MIC) OF CHALCONE IMINE DERIVATIVES (**4a-e**) AGAINST *Staphylococcus aureus*

Compound	Zone of inhibition (mm)		
	50 µg/mL	100 µg/mL	150 µg/mL
4a	17	24	27
4b	19	24	26
4c	15	21	24
4d	16	20	22
4e	21	26	26
Amoxicillin (100 µg/mL)	–	28	–
Cefixime (100 µg/mL)	–	28	–
Control	–	–	–

Conclusion

We documented a one-pot synthesis of hydrazone derivatives incorporating fluoro and methylene dioxy moiety. We have demonstrated a relatively efficient catalytic method for the one-pot synthesis of chalconeimine derivatives catalyzed successfully *via* ZnO nanoparticles. This method gives many benefits consisting of avoidance of dangerous organic solvents, high yield, quick reaction time, simple work-up method, ease of separation and recyclability of the catalyst. Docking analysis of all of the 5 chalcone imine derivatives (**4a-e**), capsules amoxillin and cefixime, co-crystallized ligands of DNA gyrase B and MTAN with the protein objectives, DNA gyrase B and MTAN produced from *S. aureus* found out important interactions among the derivatives and enzymes. The docking research with the structure of chalcone imine derivatives show that the compound **4a**, **4b** and **4e** being small and compact molecule are positioned deep into the energetic website online of the MTAN and DNA gyrase B produced from *S. aureus*. With a view to compare chalconeimine derivatives for its performance standard tablets amoxicillin, cefixime and co crystallized ligands methyl ((5-(4-(4-hydroxypiperidin-1-yl)-2-phenylthiazol-5-yl)-1*H*-pyrazol-3-yl)methyl)carbamate and formycin A is covered in our docking studies. The antibacterial interest of synthesized novel chalcone-imine derivatives were correctly screened towards Gram-nice *S. aureus* bacterial strain. Most of those compounds display slight antibacterial activity comparable with to marketable compounds. The zone of inhibition of tested compounds indicates, the chalconeimine derivative **4a**, **4b** and **4e** encompass powerful bio-sports towards bacterial pressure. Due to the robust bio-pastime of our synthesized hydrazones can be further allowed to strive different bio-activities in opposition to a number of diseases and this paintings may be valuable for further research in terms of toxicity effect and amount structural activity relationship (QSAR) to improve their organic and pharmacological researches.

CONFLICT OF INTEREST

The authors declare that there is no conflict of interests regarding the publication of this article.

REFERENCES

1. C.L. Miranda, J.F. Stevens, V. Ivanov, M. McCall, B. Frei, M.L. Deinzer and D.R. Buhler, *J. Agric. Food Chem.*, **48**, 3876 (2000); https://doi.org/10.1021/jf0002995.
2. M. Liu, P. Wilairat and L.M. Go, *J. Med. Chem.*, **44**, 4443 (2001); https://doi.org/10.1021/jm0101747.
3. G.S. Viana, M.A. Bandeira and F. Matos, *Phytomedicine*, **10**, 189 (2003); https://doi.org/10.1078/094471103321659924.
4. V. Rangari, V.N. Gupta and C.K. Atal, *Indian J. Pharm. Sci.*, **52**, 158 (1990).
5. F. Epifano, S. Genovese, L. Menghini and M. Curini, *Phytochemistry*, **68**, 939 (2007); https://doi.org/10.1016/j.phytochem.2007.01.019.
6. Nissan Chemical Industries Ltd., Japan Kokai Tokkyo Koho Japan Patent 58,08,035 (1983); *Chem. Abstr.*, **98**, 178947a (1983).
7. K. Bowden, P.A. Dal and C.K. Shah, *J. Chem. Res. (S)*, **12**, 2801 (1990); *Chem. Abstr.*, **114**, 160570m (1991).
8. V.M. Gaurav and D.B. Ingle, *J. Indian Chem.*, **25B**, 868 (1986).
9. L.C. Manchester, B. Poeggeler, F.L. Alvares, G.B. Ogden and R.J. Reiter, *Cell Mol. Biol. Res.*, **41**, 391 (1995).
10. H.W. Boucher, G.H. Talbot, J.S. Bradley, J.E. Edwards, D. Gilbert, L.B. Rice, M. Scheld, B. Spellberg and J. Bartlett, *Clin. Infect. Dis.*, **48**, 1 (2009); https://doi.org/10.1086/595011.
11. J. Kluytmans, A. van Belkum and H. Verbrugh, *Clin. Microbiol. Rev.*, **10**, 505 (1997); https://doi.org/10.1128/CMR.10.3.505.
12. M.J. Kuehnert, H.A. Hill, B.A. Kupronis, J.I. Tokars, S.L. Solomon and D.B. Jernigan, *Emerg. Infect. Dis.*, **11**, 868 (2005); https://doi.org/10.3201/eid1106.040831.
13. R.M. Klevens, M.A. Morrison, J. Nadle, S. Petit, K. Gershman, S. Ray, L.H. Harrison, R. Lynfield, G. Dumyati, J.M. Townes, A.S. Craig, E.R. Zell, G.E. Fosheim, L.K. McDougal, R.B. Carey and S.K. Fridkin, *JAMA*, **298**, 1763 (2007); https://doi.org/10.1001/jama.298.15.1763.
14. M. Diefenbeck, U. Mennenga, P. Guckel, A.H. Tiemann, T. Muckley and G.O. Hofmann, *Z. Orthop. Unfall.*, **149**, 336 (2011); https://doi.org/10.1055/s-0030-1270952.
15. J.L. Wang, S.P. Tseng, P.R. Hsueh and K. Hiramatsu, *Taiwan Emerg. Infect. Dis.*, **10**, 1702 (2004).
16. J. Ruiz, *J. Antimicrob. Chemother.*, **51**, 1109 (2003); https://doi.org/10.1093/jac/dkg222.
17. J.A. Sutcliffe, T.D. Gootz and J.F. Barrett, *Antimicrob. Agents Chemother.*, **33**, 2027 (1989).
18. C.B. Anfinsen, J. Edsall and F. Richards, Advances in Protein Chemistry, Academic Press: (Google eBook), vol. 38 (1986).
19. N. Parveen and K.A. Cornell, *Mol. Microbiol.*, **79**, 7 (2011); https://doi.org/10.1111/j.1365-2958.2010.07455.x.
20. K.K.W. Siu, J.E. Lee, G.D. Smith, C. Horvatin-Mrakovcic and P.L. Howell, *Acta Crystallogr. Sect. F Struct. Biol. Cryst. Commun.*, **64**, 343 (2008); https://doi.org/10.1107/S1744309108009275.
21. J.W. Miller, M.R. Nadeau, J. Smith, D. Smith and J. Selhub, *Biochem. J.*, **298**, 415 (1994); https://doi.org/10.1042/bj2980415.
22. S. Schauder, K. Shokat, M.G. Surette and B.L. Bassler, *Mol. Microbiol.*, **41**, 463 (2001); https://doi.org/10.1046/j.1365-2958.2001.02532.x.
23. X. Chen, S. Schauder, N. Potier, A. Van Dorsselaer, I. Pelczer, B.L. Bassler and F.M. Hughson, *Nature*, **415**, 545 (2002); https://doi.org/10.1038/415545a.
24. J.H. Clark, *Pure Appl. Chem.*, **73**, 103 (2001); https://doi.org/10.1351/pac200173010103.
25. V.J. Mohanraj and Y. Chen, *Trop. J. Pharm. Res.*, **5**, 561 (2006); https://doi.org/10.4314/tjpr.v5i1.14634.
26. G.M. Morris, R. Huey, W. Lindstrom, M.F. Sanner, R.K. Belew, D.S. Goodsell and A.J. Olson, *J. Comput. Chem.*, **30**, 2785 (2009); https://doi.org/10.1002/jcc.21256.
27. O. Trott and A.J. Olson, *J. Comput. Chem.*, **31**, 455 (2010); https://doi.org/10.1002/jcc.21334.
28. F.C. Bernstein, T.F. Koetzle, G.J.B. Williams, E.F. Meyer Jr., M.D. Brice, J.R. Rodgers, O. Kennard, T. Shimanouchi and M. Tasumi, *J. Mol. Biol.*, **112**, 535 (1977); https://doi.org/10.1016/S0022-2836(77)80200-3.
29. D. Kaushik, S.A. Khan, G. Chawla and S. Kumar, *Eur. J. Med. Chem.*, **45**, 3943 (2010); https://doi.org/10.1016/j.ejmech.2010.05.049.
30. S. Han, F.-F. Zhang, X. Xie and J.-Z. Chen, *Eur. J. Med. Chem.*, **74**, 73 (2014); https://doi.org/10.1016/j.ejmech.2013.12.018.
31. S.-Y. Pung, W.-P. Lee and A. Aziz, *Int. J. Inorg. Chem.*, **2012**, 1 (2012); https://doi.org/10.1155/2012/608183.
32. B.D. Culity, Elements of X-Ray Diffraction, Addison-Wesley: USA, edn 2 (1987).
33. P. Bhattacharyya, K. Pradhan, S. Paul and A.R. Das, *Tetrahedron Lett.*, **53**, 4687 (2012); https://doi.org/10.1016/j.tetlet.2012.06.086.
34. S. Farhadi and Z. Babazadeh Maleki, *Acta Chim. Slov.*, **53**, 72 (2006).
35. K.A. Ohemeng, B.L. Podlogar, V.N. Nguyen, J.I. Bernstein, H.M. Krause, J.J. Hilliard and J.F. Barrett, *J. Med. Chem.*, **40**, 3292 (1997); https://doi.org/10.1021/jm9701583.